V. Conclusion

The model of Fig. 3 can be used to explain and analyze the operation of the loop-gain modulator. The concept of this modulator offers a new approach to amplitude modulation. The linearity of modulation for either the class-A or class-C stage is excellent for modulation indexes that approach unity. This linearity is comparable to that of the collector modulation circuit. The modulation source power requirement is minimized by placing this source in the base circuit of the transistor. The power requirement for the modulation source is two to three orders of magnitude less than that of the collector modulation circuit.

References

[1] P. M. Chirlian, *Analysis and Design of Integrated Electronic Circuits*. New York: Harper and Row, 1981, chap. 20.

[2] H. L. Krauss, C. W. Bostian, and F. H. Raab, *Solid State Radio Engineering*. New York: Wiley, 1980, chaps. 8 and 13.

[3] D. J. Comer, *Modern Electronic Circuit Design*. Reading, MA: Addison-Wesley, 1976, chap. 14.

[4] D. J. Comer, M. L. Christiansen, and D. K. Fox, "The loop-gain modulator: A new class of linear amplitude modulators," *IEEE Trans. Circuits Syst.*, vol. CAS-34, pp. 1161–1164, 1987.

[5] N. R. Draper and H. Smith, *Applied Regression Analysis*. New York: Wiley, 1966.

[6] D. J. Comer and R. Herron, "A class-C loop-gain amplitude modulator," *IEEE Trans. Circuits Syst.*, vol. 36, pp. 159–162, 1989.

An Improved Correlated Double Sampling Circuit for Low Noise Charge-Coupled Devices

H. M. WEY AND W. GUGGENBÜHL

Abstract—**Correlated double sampling (CDS) is a widespread noise reduction method for the discrete-time output signals of charge-coupled devices (CCD). This paper describes an improved CDS circuit with noise performance superior to the classical one, at the hardware expense of only one additional FET switch. By allowing a smaller noise bandwidth, the total noise contribution from the video amplifier can be reduced, and pixel crosstalk and kTC noise will even be completely eliminated. It is shown that the proposed approach is close to optimum filtering.**

I. Introduction

Correlated double sampling (CDS) is a well-known noise reduction method for charge-coupled devices (CCD) signals, and its application is indispensable for low light level (LLL) imaging. The basic intention of CDS has been the elimination of the kTC noise in the CCD output diffusion and the reduction of the $1/f$ noise generated in the front-end video amplifier [1].

CDS, however, doubles the noise power of the broadband (i.e., white) noise, since the two samples taken and subtracted in each pixel clock cycle are not correlated. A step towards the reduction of the broadband noise is the introduction of a low-pass filter (LPF) preceding the CDS [2]. This filter reduces the broadband noise contribution at the expense of pixel crosstalk and a lower kTC-noise and $1/f$ noise suppression.

Manuscript received September 5, 1989; revised July 25, 1990. This paper was recommended by Associate Editor D. Graupe.

The authors are with the Institut fuer Elektronik, Swiss Federal Institute of Technology, CH-8092 Zurich, Switzerland.

IEEE Log Number 9039233.

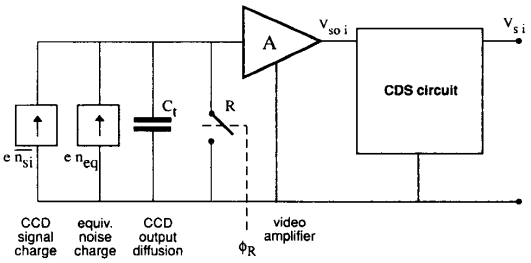

Fig. 1. Block diagram of the CCD signal processing path with signal source and equivalent noise source.

In recent papers, further methods of low-noise CCD signal recovery have been presented. One solution [3] is related to the classical *CR-RC*-filtering in nuclear particle detectors. This circuit is advantageous in view of the hardware expense and speed. The occurring "differential" pixel crosstalk might be desired in some cases to enhance the display resolution (high frequency peaking) but is unsuitable for computerized picture processing. The signal-to-noise ratio (SNR) of this method is far from optimum. Furthermore, it is difficult to sample the small differentiated signal peaks appearing at the output of the high-pass filter section.

Another method uses the classical synchronous detector for CCD signal recovery [4]. Its drawbacks are the need for a higher order filter, and only the partial elimination of the kTC noise. One advantage, however, could be the continuous-time analog video signal output in applications where no further digital signal processing is required.

In this paper, a CDS circuit will be described, where the filter bandwidth can be reduced by a factor of 4 or more with respect to the classical CDS method [2] without worsening kTC noise and pixel crosstalk performance, and thus improving the overall noise performance. It is shown that this approach corresponds to a nearly optimum filtering of a CCD output signal to get almost the maximum attainable SNR.

Note that the stochastic noise generated in the sensor elements and transfer registers of the CCD (i.e., photon noise, dark current noise, transfer noise, charge transfer inefficiency) cannot be reduced by any CDS-type processing. The correction of the CCD fixed-pattern noise is another prerequisite for LLL imaging and can be performed with deterministic methods.

II. Signal and Noise Modeling of the CCD Output Stage

The signal and noise contributions from the CCD front-end video amplifier are treated in detail in [8].

Signal Model

The CCD output stage is modeled in Fig. 1. At each pixel clock interval a charge packet $\overline{q_{si}} = e\overline{n_{si}}$ is fed to the capacitance C_t where $\overline{n_{si}}$ denotes the mean number of electrons of charge e from pixel i and C_t the total capacitance of the CCD output node (i.e., CCD output diffusion and stray capacitances). C_t is discharged by the reset switch R at the end of each pixel clock cycle. It is necessary to raise the signal to a level in the range of several volts prior to CDS processing. With a voltage gain A of the video amplifier, and assuming sufficient bandwidth, the

0098-4094/90/1200-1559$01.00 ©1990 IEEE

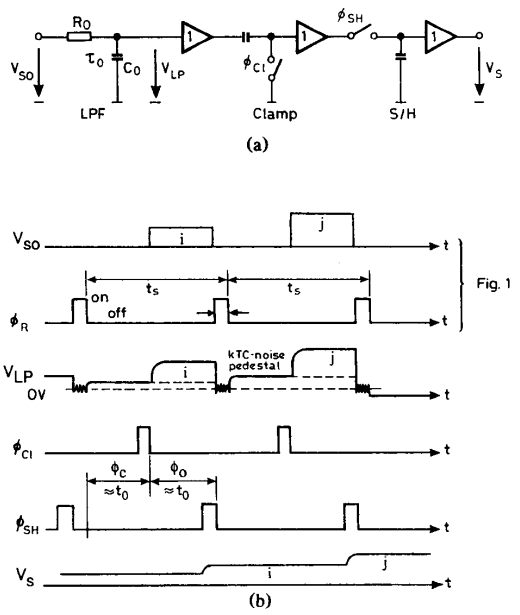

Fig. 2. Classical CDS (CDS1). (a) Circuit. (b) Timing.

output from pixel i is a voltage pulse of height

$$V_{soi} = \overline{n_{si}} eA / C_t \tag{1}$$

which feeds the CDS circuit.

Noise Model

The following noise components appear at the video amplifier output:

1) The (double-sided) white noise power spectral density N_W [V^2/Hz] due to thermal noise of the FET channel and the ohmic resistors.

2) The noise power spectral density

$$N_f(f) = N_{f1} / |f|^{\alpha} \tag{2}$$

of the FET $1/f$ noise, where N_{f1} [V^2] represents the spectral density at unity frequency and α is close to 1.

3) A dc leakage current (i.e., bias current) I_o is integrated on C_t; its stochastic nature results in a so-called bias noise with a variance of the number of charge carriers on C_t

$$\overline{n_d^2} = \overline{n_d} = |I_o| t_o / e \tag{3}$$

which corresponds according to Poisson distribution to the mean number of charge carriers $\overline{n_d}$ integrated on C_t during a time interval t_o. The resulting variance at the video amplifier output is

$$\overline{v_d^2} = \overline{n_d} (eA / C_t)^2. \tag{4}$$

4) The reset switch R generates kTC noise [5], which is due to the ohmic channel resistance. The fluctuating charge on the capacitor C_t is frozen when the switch opens. The respective kTC noise is a discrete-time stochastic signal with uncorrelated succeeding samples and the variance [5]

$$\overline{v_r^2} = A \text{ kT} / C_t. \tag{5}$$

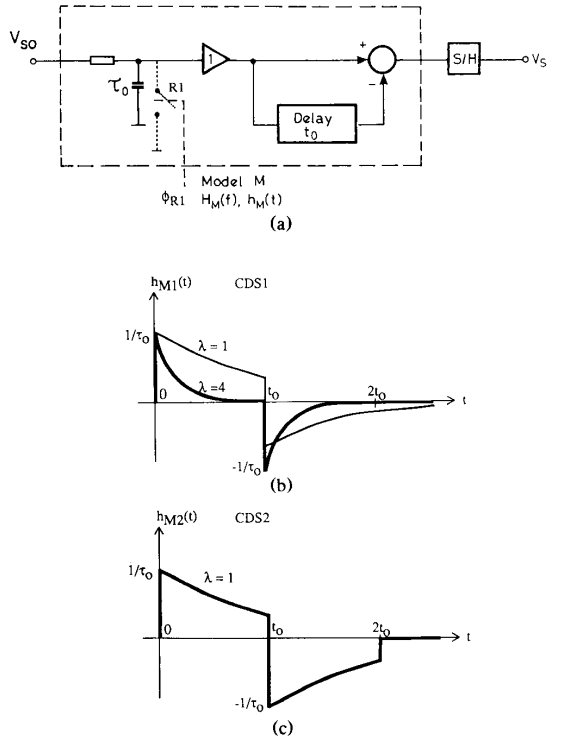

Fig. 3. (a) Model of the clamp as a transversal filter (dashed part valid for CDS2). (b) Impulse response $h_{M1}(t)$ of CDS1. (c) Impulse response $h_{M2}(t)$ of CDS2.

III. Classical CDS Circuit (CDS1)

A detailed description of the classical CDS concept is given in [1] and [5]. Basically, CDS acts as a dc restorer or clamp operated at pixel clock frequency. kTC noise, which is usually the dominant noise source in the CCD output stage, can be eliminated by this clamp operation. In addition, all low-frequency noise sources (i.e., dc-offset, low-frequency part of the $1/f$ noise, bias noise) will be reduced by CDS as well.

The CDS circuit and its associated timing is shown in Fig. 2. The pixel clock interval t_s is divided into the reference or clamp phase ϕ_c and the signal phase ϕ_o, each of duration

$$t_o = (t_s - t_r)/2 \tag{6}$$

while a small time slot t_r within t_s is used to discharge C_t with the reset switch R.

The first-order LPF with time constant $\tau_o = R_o C_o$ reduces the high-frequency noise components. With respect to the first-order LPF, no further noise reduction is possible by use of a higher order LPF because the rather small additional reduction of the noise bandwidth will not compensate for the increase of the signal rise-time.

Our mathematical analysis of the CDS noise performance uses the model of Fig. 3(a) [6], incorporating the LPF and a first-order transversal filter built with a delay line of delay t_o. This circuit allows us to calculate the noise performance with classical continuous-time methods. The following sample/hold circuit (S/H) changes the noise spectral density distribution; however, it does not alter the total output noise power.

The LPF has an impulse response

$$h_{LP}(t) = U(t)\exp(-t/\tau_o)/\tau_o, \qquad U(t)\text{: unit step function.} \tag{7}$$

The impulse response $h_{M1}(t)$ of the complete CDS model M (see Fig. 3) excluding the S/H yields the convolution

$$\begin{aligned} h_M(t) &= h_{M1}(t) = h_{LP}(t)*(\delta(t)-\delta(t-t_o)) \\ &= h_{LP}(t) - h_{LP}(t-t_o) \\ &= \begin{cases} 0 \\ \exp(-t/\tau_o)/\tau_o \\ (1-\exp(-t_o/\tau_o)) \\ \cdot\exp(-t/\tau_o)/\tau_o \end{cases} \quad \text{for} \quad \begin{cases} t<0 \\ 0 \leqslant t \leqslant t_o \\ t_o < t \end{cases} \end{aligned} \tag{8}$$

which is shown in Fig. 3(b). Its associated transfer function is

$$\begin{aligned} H_M(j\omega) &= H_{M1}(j\omega) \\ &= j2\exp(-j\omega t_o/2)\sin(\omega t_o/2)/(1+j\omega\tau_o). \end{aligned} \tag{9}$$

Signal Transfer of CDS

As can be seen from Fig. 2, the signal pulse V_{soi} of pixel i occurs during a time interval ϕ_o. The respective CDS output voltage V_{si} at sampling time t_o after the transfer of a charge packet to the CCD output diffusion C_t is the convolution of the signal pulse with the CDS impulse response $h_{M1}(t)$ and yields

$$V_{si} = V_{soi}\int_0^{t_o} h_{M1}(t)\,dt = V_{soi}(1-\exp(-\lambda)) \tag{10}$$

where

$$\lambda = t_o/\tau_o. \tag{11}$$

Noise Transfer of CDS

1) White Noise: With $B_n = 1/(4\tau_o)$ denoted as the LPF equivalent white-noise bandwidth, the variance of the LPF output due to a white-noise input source with power spectral density N_W is

$$\overline{v_{LP}^2} = 2N_W B_n = N_W/(2\tau_0). \tag{12}$$

N_W applied to a network characterized by $H_M(j\omega)$ or $h_M(t)$, respectively, yields at its output

$$\overline{v_W^2} = 2N_W\int_0^\infty |H_M(j\omega)|^2\,df = N_W\int_0^\infty |h_M(t)|^2\,dt. \tag{13}$$

With (8) and (9) inserted in (13), we get

$$\overline{v_{W1}^2} = N_W(1-\exp(-\lambda))/\tau_o = \overline{v_{LP}^2}2(1-\exp(-\lambda)). \tag{14}$$

To maintain sufficient kTC noise suppression and low pixel crosstalk, a high value of λ is required. With this condition met, the output noise power is doubled with respect to the noise power output of the LPF alone, because the two noise samples gathered after ϕ_c and ϕ_o are not correlated.

2) 1/f Noise ($\alpha = 1$): The output variance with $1/f$ noise spectral density $N_f(f) = N_{f1}/|f|$ applied at the CDS input is treated in [6], [7] and reads [7]

$$\overline{v_{f1}^2} = 4N_{f1}(0.577+\ln\lambda), \qquad \text{for } \lambda > 3. \tag{15}$$

Our own calculations following a different method [8] confirm this result. The variance is dependent only on the ratio parameter λ and not on the absolute pixel clock frequency $f_s = 1/t_s$ itself.

3) Bias Noise: The output variance for the bias noise at the CDS input yields [8]

$$\overline{v_b^2} = \overline{v_d^2}\int_0^\infty |h_I(t)|^2\,dt \tag{16}$$

where

$$h_I(t) = \int_{-\infty}^t h_M^2(t)\,dt. \tag{17}$$

With (9) inserted in (17), (16) yields

$$\overline{v_{b1}^2} = \overline{v_d^2}(1-(1-\exp(-\lambda))/\lambda). \tag{18}$$

4) kTC Noise: Because of the LPF in the CDS signal path, the kTC noise cannot be eliminated completely by the CDS circuit. The variance due to kTC noise reads [8]

$$\overline{v_{\text{kTC}}^2} = \overline{v_r^2}\left(\int_0^{2t_o} h_M(t)\,dt\right)^2. \tag{19}$$

With (9) inserted in (19), we get

$$\overline{v_{\text{kTC1}}^2} = \overline{v_r^2}\exp(-2\lambda)(1-\exp(-\lambda))^2. \tag{20}$$

5) Pixel Crosstalk: Apart from the degradation of the charge pattern in the CCD channel, which is not treated here, pixel crosstalk stems from the signal dispersion in the LPF of the CDS section. It results in a degradation of the CCD imager modulation transfer function. Assuming a worst case that all previous pixels have delivered the maximum charge to the output diffusion C_t, namely the saturation charge $\overline{n_{ss}}$ of the CCD, the resulting crosstalk voltage at the CDS output reads

$$\overline{v_c} = \overline{n_{ss}}(eA/C_t)\sum_{i=0}^{\infty}\int_{t_s(i+1)}^{t_s(i+1)+t_o} h_M(t)\,dt. \tag{21}$$

With (9) inserted in (21), we get

$$\overline{v_{c1}} = -\overline{n_{ss}}(eA/C_t)\exp(-\lambda)(1+\exp(-\lambda)). \tag{22}$$

In order to obtain negligible pixel crosstalk and a good kTC-noise rejection, a value of

$$\lambda \geqslant 4 \tag{23}$$

is required [2]. With this condition met, however, the white noise and $1/f$-noise contributions will raise significantly.

IV. Novel Improved CDS-Circuit (CDS2)

In further sections, the classical CDS and the improved CDS circuit are designated as CDS1 and CDS2, respectively. In the CDS2 circuit, the LPF bandwidth can be reduced with respect to CDS1 in order to diminish the contribution of the broadband noise sources, without increasing kTC noise and pixel crosstalk. This is achieved by truncating the impulse response $h_{M2}(t)$ in a way that no tails overlap into the next pixel clock interval.

For a complete elimination of the kTC noise, the positive and negative area of $h_{M2}(t)$ must be of equal value. Furthermore, in order to get a small attenuation of the signal, the absolute area under $h_{M2}(t)$ during the signal phase ϕ_o should be made as large as possible.

A slight modification of the circuit of Fig. 2(a) meets these requirements by introducing a reset switch $R1$ across the LPF capacitor C_o as shown in Fig. 4(a). If timed according to Fig.

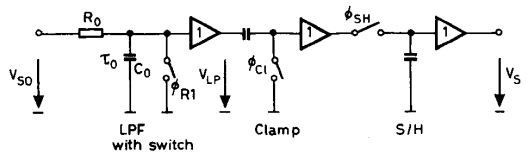

(a)

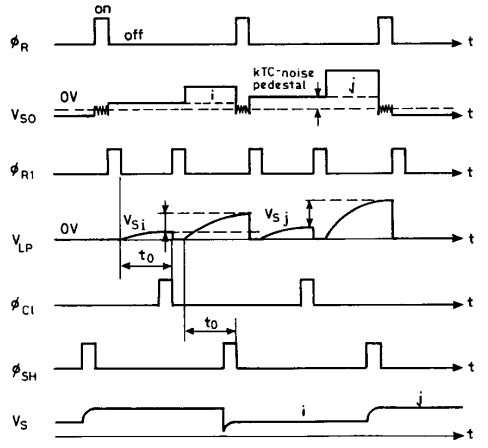

(b)

Fig. 4. CDS2. (a) Circuit. (b) Timing.

4(b) the following impulse response results (see Fig. 3(c)):

$$h_M(t) = h_{M2}(t) = \begin{cases} 0 & \text{for } \begin{cases} t<0,\ 2t_o<t \\ 0\leqslant t\leqslant t_o \\ t_o<t\leqslant 2t_o. \end{cases} \\ \exp(-t/\tau_o)/\tau_o \\ -\exp(-(t-t_o)/\tau_o)/\tau_o \end{cases} \quad (24)$$

The associated transfer function is

$$H_M(j\omega) = H_{M2}(j\omega) = H_{M1}(j\omega)(1-\exp(-j\omega t_o)\exp(-\lambda)). \quad (25)$$

For large values of λ, the system performance of CDS2 and CDS1 will be the same with respect to white, $1/f$, and bias noise. It will be shown, however, that with CDS2 an optimum value of λ for maximum SNR exists in the region of λ about 1.

Signal Transfer

Because of the integration interval $(0, t_o)$ in (10), the same signal output voltage as with CDS1 holds.

Noise Transfer

1) White Noise: Following (13) with (24) and (25), the variance at the CDS2 output yields

$$\overline{v_{W2}^2} = 2N_W B_n 2(1-\exp(-2\lambda)) = N_W(1-\exp(-2\lambda))/\tau_o. \quad (26)$$

This equation describes the transient noise power across the capacitor C_o of the LPF (see Fig. 4(a)) at time t_o after having reset it by $R1$ [5] and multiplied by a factor of 2 because of the clamp, since for white noise the samples after ϕ_c and ϕ_o are not correlated and thus their noise power adds.

2) 1/f-Noise ($\alpha = 1$): For $\lambda \geqslant 3$, the variance of CDS1 and CDS2 yields the same and thus (15) is valid. For values of $\lambda \leqslant 0.3$, CDS2 behaves like a differential integrator (see Fig. 10(b)) and the variance according to [7] is

$$\overline{v_{f2}^2} = N_{f1}\lambda^2 8\ln 2. \quad (27)$$

3) Bias Noise: Application of (16) and (17) results in the output variance for the bias noise

$$\overline{v_{b2}^2} = \overline{v_d^2}(1+\exp(-2\lambda)-(1-\exp(-2\lambda))/\lambda). \quad (28)$$

4) kTC Noise and Pixel Crosstalk: Applying (19) and (21) with the (truncated) $h_{M2}(t)$ results in a complete elimination of these noise contributions.

Hardware Requirements for CDS2

The proposed improved CDS2 uses only one additional switch as compared with the conventional CDS1. In high-speed applications, the associated additional reset time of the LPF may be disadvantageous. Since only a few switching actions are allowed in the signal processing circuit to get video speed [5], [9], a tradeoff between processing speed and low-noise performance exists. For this reason, the field of applications of the improved CDS2 lies in LLL imaging rather than in very high-speed CCD video operation.

For exact cancelling of dc offset and kTC noise, the duration of the reference phase ϕ_c and signal phase ϕ_o of the impulse response must be of equal length t_o. Furthermore, the overall filter characteristic has to be of first-order, which implies that the poles of the video amplifiers may not be dominant.

An all digital CCD signal processing scheme with the same filter characteristics has been developed, which is presented in [9].

V. Comparison of the Two CDS Systems

A signal amplification factor A_s that refers the signal output voltage V_{si} to the number of electrons $\overline{n_{si}}$ of the CCD charge packet i is defined with (1) and (10) according to

$$A_s(\lambda) = V_{si}/\overline{n_{si}} = C_t(1-\exp(-\lambda))/eA. \quad (29)$$

Equivalent Noise Charge Carriers at the CCD Output Diffusion

In order to set the occurring distortions (i.e., noise, pixel crosstalk) in relation to the signal charge, they will be expressed in terms of equivalent signal electrons n_{eq} at the CCD output diffusion C_t, i.e., the respective CDS output voltage $v(\lambda, t_o)$ is normalized according to

$$n_{eq} = v(\lambda,t_o)/A_s(\lambda) = v(\lambda,t_o)C_t/(eA(1-\exp(-\lambda))). \quad (30)$$

The respective results are listed in Table I and plotted in Figs. 5–8 for CDS1 and CDS2 as a function of λ. Remember that a value λ of about 4 or greater (i.e., high relative bandwidth) is required in a classical CDS1 system if pixel crosstalk and kTC-noise contribution have to be held at a reasonable low value (see Fig. 8). In the CDS2 system, a value of λ close to 1 (i.e., a much smaller LPF bandwidth) is a reasonable choice. Reducing λ even more attenuates the signal level without further noise reduction. Design center regions for both circuits CDS1 and CDS2, respectively, are marked in Figs. 5–7. The noise reduction of CDS2 against CDS1 depends on the relative magnitude

TABLE I
EQUIVALENT NUMBER OF CHARGE CARRIERS AT THE CCD OUTPUT DIFFUSION C_t. THE INDEXES 1,2 REFER TO CDS1 AND CDS2, RESPECTIVELY

signal charge	$\overline{n_s} = 0 \ldots \overline{n_{ss}}$
saturation charge	$\overline{n_{ss}} = (0.2 \ldots 1)\ 10^6$ e
noise components:	
white noise	$\overline{n_{w1}^2} = (C_t/eA)^2\ N_w\ \lambda/(t_o(1-\exp(-\lambda)))$
	$\overline{n_{w2}^2} = (C_t/eA)^2\ N_w\ \lambda(1+\exp(-\lambda))/(t_o(1-\exp(-\lambda)))$
(Fig.5)	
1/f-noise	$\overline{n_{f1}^2} = (C_t/eA)^2\ 4\ N_{f1}\ (0.577+\ln\ \lambda)/(1-\exp(-\lambda))^2$ for $\lambda>3$
(Fig.6)	$\overline{n_{f2}^2} = (C_t/eA)^2\ N_{f1}\ \lambda^2 8\ \ln 2/(1-\exp(-\lambda))^2$ for $\lambda<0.3$
bias-noise	$\overline{n_{b1}^2} = \overline{n_d}\ (1-(1-\exp(-\lambda))/\lambda)/(1-\exp(-\lambda))^2$
(Fig.7)	$\overline{n_{b2}^2} = \overline{n_d}(1+\exp(-2\lambda)-(1-\exp(-2\lambda))/\lambda)/(1-\exp(-\lambda))^2$
kTC-noise	$\overline{n_{kTC1}^2} = kTC_t \exp(-2\lambda)/e^2$
(Fig.8)	$\overline{n_{kTC2}^2} = 0$
pixel crosstalk	$\overline{n_{c1}} = -\overline{n_{ss}}\ \exp(-\lambda)/(1+\exp(-\lambda))$
(Fig.8)	$\overline{n_{c2}} = 0$

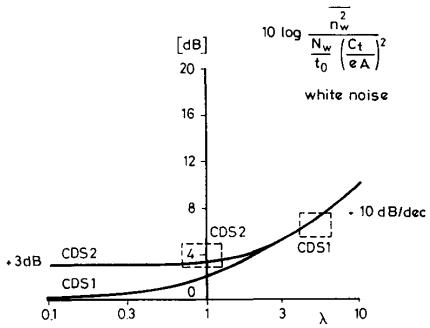

Fig. 5. Equivalent noise charge carriers n_W on C_t normalized to white noise spectral density N_W at the CDS input as a function of λ.

of the different noise sources. For a typical CCD imager system, this reduction lies between 3–8 dB. The higher limit is valid if pixel crosstalk and kTC noise is considered.

VI. MEASUREMENTS

Measurements have been carried out with a Fairchild CCD110F linear CCD imager as a signal source. This device incorporates an additional identical output stage (i.e., CCD output diffusion, reset switch, and MOSFET source follower), but has no CCD channel in front of it. This compensation amplifier allows noise measurements of the CCD output stage alone, without introducing noise charge from the CCD channel. Furthermore, the CCD shift clock was held at dc level to avoid capacitive pickup to the compensation amplifier.

Because of the low capacitance of the CCD output diffusion C_t, a step in the range of 100 mV occurs at the source follower output due to the clock feedthrough of the reset switch R. To avoid a saturation of the video amplifier, this feedthrough has to be compensated [8], especially for LLL imaging where a high video amplifier gain is required.

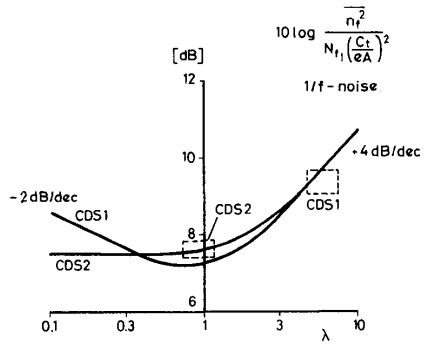

Fig. 6. Equivalent noise charge carriers n_f on C_t for $1/f$ noise normalized to spectral density N_{f1} at the CDS input as a function of λ.

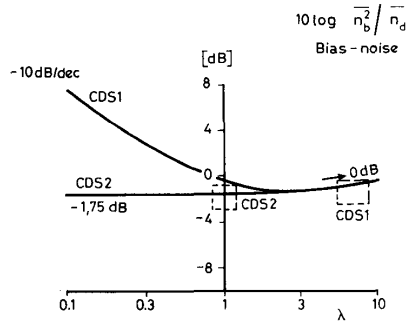

Fig. 7. Normalized equivalent noise charge carriers n_b for bias noise as a function of λ.

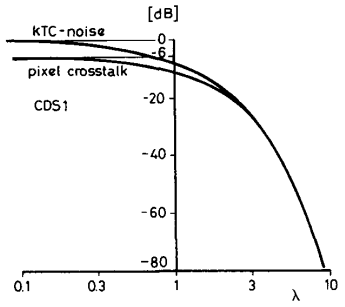

Fig. 8. Normalized kTC noise suppression $n_{kTC1}e/(kTC_t)^{1/2}$ and pixel crosstalk $n_{c1}/\overline{n_{ss}}$ for CDS1 as a function of λ.

The following data were measured for the experimental circuit:

$$C_t = 0.18 \text{ pF}$$
$$A = 1000$$
$$N_W = 52\ (\mu\text{V})^2/\text{Hz}$$
$$N_{f1} = 68\ (\text{mV})^2$$
$$I_o = 5 \text{ fA}, 25°\text{C}.$$

The equivalent number of charge carriers corresponding to the output noise of the CCD output stage stage are shown in Fig. 9 as a function of the pixel clock frequency f_s.

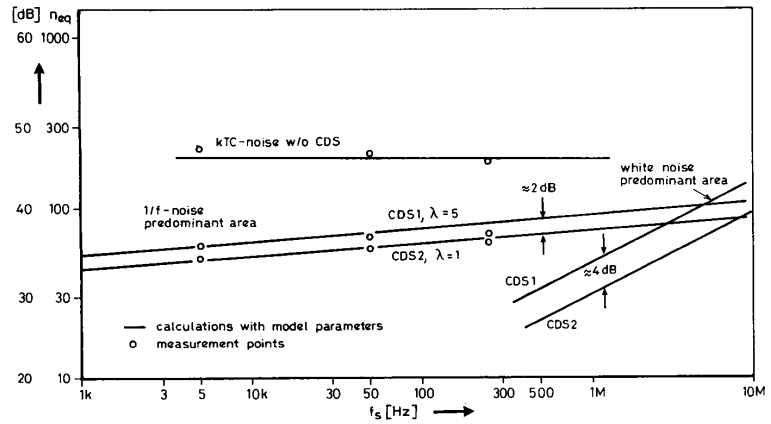

Fig. 9. Equivalent noise charge carriers n_{eq} on C_t calculated from the measurements with a Fairchild CCD110F linear CCD imager as a function of pixel clock frequency f_s.

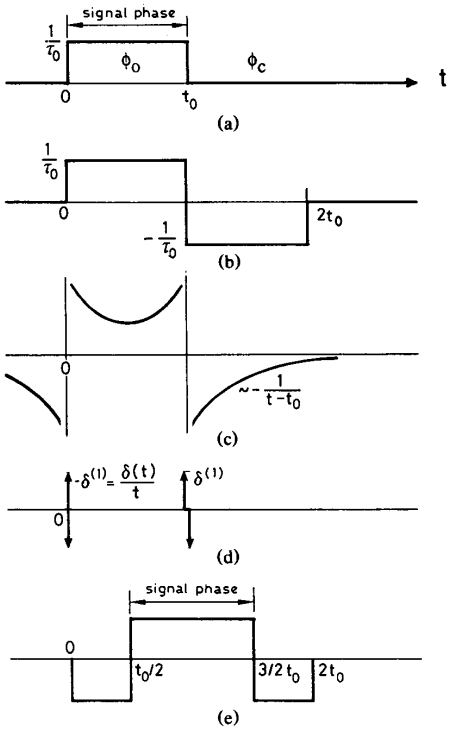

Fig. 10. Impulse response of different filters. (a) Optimum filter for white noise. (b) Optimum filter for white noise and kTC noise. (c) Optimum filter for $1/f$ noise and kTC noise. (d) Optimum filter for bias noise and kTC noise. (e) Modified (d) for the floating gate amplifier.

CDS2 always shows the better noise performance than the conventional CDS1. In the frequency range of measurement where the $1/f$ noise is dominant, the dependence of the noise level from the pixel clock frequency f_s is due to α different from 1 (see (2)). In accordance with Fig. 6, here the noise reduction of CDS2 against CDS1 is moderate. A more efficient noise reduction can be achieved in a range of pixel clock frequency f_s where white noise is predominant. The additional improvement of pixel crosstalk and kTC-noise reduction has not been considered with the reported experiments.

VII. Comments on CDS and Optimized Filtering

According to the theory of matched filters, the optimum SNR for a signal-step in the presence of white noise is performed by an integrator. For a unit step of duration t_o, the integration has to be limited to the interval t_o. The respective impulse function is shown in Fig. 10(a). The suppression of kTC noise and dc offset, however, requires a dc-free impulse function of the respective signal processing path. The impulse response of CDS1 has nearly zero dc content in the time interval $(0, 2t_o)$ if $\lambda = t_o/\tau_o \gg 1$, meaning a large relative LPF bandwidth. For smaller bandwidths the impulse response extends to the next pixel interval, and pixel crosstalk and kTC noise are not completely eliminated. The impulse response of the CDS2 system has a mean dc content of zero and disappears outside the time internal $(0, 2t_o)$ and therefore eliminates the pixel crosstalk for all values of λ. In both cases, the filtering with respect to white noise is not optimal. However, with the requirement of a dc-free impulse response, the differential-integrator function according to Fig. 10(b) is an optimal solution.

Applying the theory of matched filters to $1/f$ and bias noise leads to the optimum filters of Fig. 10(c) and 10(d). They show that information on noise has to be gathered before and after the presence of the signal pulse. This could not be performed with a CCD floating diffusion amplifier since the reset process with the associated kTC noise prohibits sampling of the noise after the signal period ϕ_o. A CCD floating gate amplifier that doesn't require a pixel reset switch R would be needed for detecting noise after the signal has left the floating gate. The impulse responses of Fig. 10(c) and 10(d) could only be approximated because of the infinite amplitudes of the δ function.

It can be shown that the CDS2 circuit with λ close to 1 approaches the "differential-integrator" of Fig. 10(b) and is a reasonably good compromise for combined white and $1/f$ noise filtering. Bias noise is usually negligible in practical circuit applications, unless the pixel clock frequency is very low. With a floating gate amplifier, modified timing, and an impulse response according to Fig. 10(e), a further reduction of the $1/f$ noise and bias noise would be possible with respect to the differential integrator of Fig. 10(b).

VIII. Summary and Conclusions

CDS is a signal processing method to reduce low frequency amplifier noise and kTC noise of sampled systems.

The different noise contributions in a typical CCD output stage and their transformation through a CDS circuit have been discussed. In a classical CDS circuit (CDS1), the bandwidth of the noise limiting filter has to be chosen rather large in order to cancel the kTC noise of the reset switch and to avoid pixel crosstalk involving large white and $1/f$ noise contributions. An improved CDS method (CDS2) has been presented that completely eliminates the pixel crosstalk and kTC-noise contribution, but maintains a low noise bandwidth. The noise reduction achieved with the new method lies in the range of 3–8 dB, with the lower limit valid for white noise and the upper limit for pixel crosstalk and kTC noise. This improved CDS circuit approaches optimum filtering of the combined noise spectrum. From the hardware point of view only one additional switch is required. The measured values with an experimental CCD output stage and CDS setup confirm the theory developed in this paper. In a more general way the theory can be extended to any switched amplitude-continuous network.

References

[1] M. W. White, D. R. Lampe, F. C. Blaha, and I. A. Mack, "Characterization of surface channel CCD image arrays at low light levels," *IEEE J. Solid-State Circuits*, vol. SC-9, pp. 1–13, Feb. 1974.

[2] R. W. Brodersen and S. P. Emmons, "The measurement of noise in buried channel charge coupled devices," in *Proc. Int. Conf. Appl. of CCD's*, pp. 331–345, San Diego, CA, 1975.

[3] P. A. Levine, "Low-noise CCD signal recovery," *IEEE Trans. Electron Devices*, vol. ED-32, pp. 1534–1537, Aug. 1985.

[4] Y. Endo, A. Furukawa, Y. Matsunaga, N. Harada, and O. Yoshida, "A new noise reduction method for CCD image sensor," in *Proc. IEE Conf. on Electro-Optic Imaging*, London, U.K., 1985.

[5] D. F. Barbe, "Imaging devices using the charge-coupled concept," *Proc. IEEE*, vol. 63, pp. 38–67, Jan. 1975.

[6] R. J. Kansy, "Response of a correlated double sampling circuit to 1/f noise," *IEEE J. Solid-State Circuits*, vol. SC-15, pp. 373–375, June 1980.

[7] G. R. Hopkinson and D. H. Lumb, "Noise reduction techniques for CCD image sensors," *J. Phys. E: Sci. Instrum.*, vol. 15, pp. 1214–1222, 1982.

[8] H. M. Wey, "Beitraege zur rauscharmen CCD-Signaldetektion," Ph.D. dissertation, Swiss Federal Institute of Technology, 1988.

[9] H. Wey, Z. Wang, and W. Guggenbühl, "Correlated triple sampling: A digital low-noise readout-method for CCD's," in *Proc. MELECON'85*, vol. II, pp. 209–212, Elsevier Science Publishers B.V., 1985.

Least Squares Inverse Polynomials and a Proof of Practical-BIBO Stability of n-D Digital Filters

P. S. REDDY, SRIDHAR R. PALACHERLA, AND M. N. S. SWAMY

***Abstract*—This paper deals with the problem of stabilizing unstable n-D practical digital filters where only one of the independent variables of the n-D signal is temporal and the other variables are spatial. We use the double least squares inverse (DLSI) method advanced by Swamy *et al.* [2] to stabilize such practical filters. We prove that the least squares inverse (LSI) of the denominator polynomial of a practical n-D digital filter will always be stable in the practical and less restrictive sense [1].**

Manuscript received October 10, 1989; revised February 19, 1990. This work was supported by the National Sciences and Engineering Research Council of Canada under Grant A-7739. This paper was recommended by Associate Editor P. H. Bauer.

The authors are with the Department of Electrical and Computer Engineering, Concordia University, Montreal, P.Q., H3G 1M8 Canada.

IEEE Log Number 9039234.

I. Introduction

The application of multidimensional (n-D) digital signal processing is in areas like seismic, sonar, and television image processing. In many situations that occur in practice, the independent variables $i_1, i_2, i_3, \cdots, i_n$ of an n-D signal $x(i_1, i_2, i_3, \cdots, i_n)$ are usually spatial variables, except that perhaps one variable, say i_j, is a temporal variable. Practically, the temporal variable is unbounded whereas the other spatial variables are bounded. In [1], using this concept of only one variable being bounded, a theorem is developed for the practical-BIBO stability of n-D discrete systems.

In [1] it is shown that the conventional-BIBO stability conditions are too restrictive for many applications. Subsequently in [2] a proof is given to show that the least squares inverse (LSI) of the denominator polynomial of a linear shift invariant n-D digital filter satisfies the practical-BIBO stability conditions given in [1]. But unfortunately, there is a flaw in their proof as reported in [3]. In their proof [2] the authors make use of the result of Robinson [4] which says that the LSI polynomial of any 1-D polynomial is always stable. But the result of Robinson is not true if the LSI selected is lacunary in the sense that it has some missing terms between the highest power term and the constant term [5].

In this paper we deal with a proof of practical-BIBO stability of n-D digital filters and show that the n-D LSI of the filter denominator polynomial satisfies the practical-BIBO stability requirement. In Section II, we present the basic definition of the LSI of an n-D polynomial. We also discuss a basic fact with respect to the stability of 1-D polynomials. In Section III, a theorem on practical-BIBO stability of n-D digital filters is given by showing that the LSI of the denominator polynomial of an n-D digital filter always satisfies the practical-BIBO stability requirement. Section IV contains the concluding remarks.

II. Some Preliminaries

This section contains some preliminary concepts and results already existing in the literature. The material presented in this section will be very useful for the easy understanding of the results presented in the subsequent sections.

Consider the transfer function of an n-D linear shift invariant digital filter

$$H(Z_1, Z_2, \cdots, Z_n) = P(Z_1, Z_2, \cdots, Z_n)/Q(Z_1, Z_2, \cdots, Z_n). \tag{1}$$

We assume that $H(Z_1, Z_2, \cdots, Z_n)$ has no nonessential singularities of the second kind on the unit polydisc.

An n-D polynomial $B(Z_1, Z_2, \cdots, Z_n)$ is the LSI polynomial of $Q(Z_1, Z_2, \cdots, Z_n)$ if $B(Z_1, Z_2, \cdots, Z_n) \approx 1/Q(Z_1, Z_2, \cdots, Z_n)$ for $|z_1| = |z_2| = \cdots = 1$. It may be noted that the coefficients b_{ij} of $B(Z_1, Z_2, \cdots, Z_n)$ are to be obtained by minimizing the error function

$$E = (1 - c_{0,0,\cdots,0})^2 + \sum_{i_1} \sum_{i_2} \cdots \sum_{i_n} c^2_{i_1, i_2, \cdots, i_n} i_1 + i_2 + \cdots + i_\eta > 0 \tag{2}$$

where c's are the coefficients of the n-D polynomial $C(Z_1, Z_2, \cdots, Z_n) = B(Z_1, Z_2, \cdots, Z_n)Q(Z_1, Z_2, \cdots, Z_n)$. Follow-

0098-4094/90/1200-1565$01.00 ©1990 IEEE